

Bayesian Modeling of Spatial Transcriptomics Data via a Modified Ising Model

Xi Jiang,^{1,2} Qiwei Li,^{3, a} and Guanghua Xiao^{2, a}

¹*Department of Statistical Science, Southern Methodist University,
3215 Daniel Avenue Dallas, TX 75275, United States*

²*Department of Population and Data Sciences, The University
of Texas Southwestern Medical Center, Dallas, TX 75390,
United States*

³*Department of Mathematical Sciences, The University of Texas at Dallas,
800 W Campell Rd, Richardson, TX 75080, United States*

arXiv:2104.13957v1 [stat.AP] 28 Apr 2021

Abstract

Recent technology breakthroughs in spatial molecular profiling (SMP), such as spatial transcriptomics sequencing, have enabled the comprehensive molecular characterization of single cells while preserving spatial and morphological information. One immediate question is how to identify spatially variable (SV) genes. Most of the current work builds upon the geostatistical model with Gaussian process that relies on the selection of *ad hoc* kernels to account for spatial expression patterns. To overcome this potential challenge and capture more spatial patterns, we introduced a Bayesian modeling framework to identify SV genes. Our model first dichotomized the complex sequencing count data into latent binary gene expression levels. Then, binary pattern quantification problem is considered as a spatial correlation estimation problem via a modified Ising model using Hamiltonian energy to characterize spatial patterns. We used auxiliary variable Markov chain Monte Carlo algorithms to sample from the posterior distribution with an intractable normalizing constant. Simulation results showed high accuracy in detecting SV genes compared with kernel-based alternatives. We also applied our model to two real datasets and discovered novel spatial patterns that shed light on the biological mechanisms. This statistical methodology presents a new perspective for characterizing spatial patterns from SMP data.

^aTo whom correspondence should be addressed. Emails: Qiwei.Li@UTDallas.edu;
Guanghua.Xiao@UTSouthwestern.edu

I. INTRODUCTION

The development of molecular profiling techniques has achieved significant breakthroughs in recent years. Molecular profiling approaches are no longer limited in exploring the structure and conformation of DNA or RNA in cells via tissue-dissociation (Femino et al., 1998), but are able to measure genomes or transcriptomic information in cells and tissues while recording their spatial information (Zhang et al., 2020). These spatial molecular profiling (SMP) techniques help to advance our understanding of gene expression and cell function, and their relationship with diseases (Shah et al., 2018). There are two major approaches for SMP techniques: sequencing-based and imaging-based (Zhang et al., 2020). Most of the imaging-based techniques, including seqFISH (Lubeck et al., 2014) and MERFISH (Chen et al., 2015), have been developed based on single-molecule fluorescence in situ hybridization (smFISH). Imaging-based SMP techniques can measure hundreds of genes on thousands of spots with subcellular spatial resolution and sample spots are randomly scattered on the two dimensional plane. Sequencing-based SMP methods capture RNA molecules by spatial barcode probes and then synthesize and sequence complementary DNA molecules (Zhang et al., 2020). Spatial transcriptomics technology (Ståhl et al., 2016) and high-definition spatial transcriptomics (HDST) (Vickovic et al., 2019) are all recently developed typical sequencing-based SMP approaches. Unlike imaging-based methods, sequencing-based techniques can measure over ten thousands of genes on single cells or on spatial locations consisting of several hundred single cells. Those sampled single cells or spatial locations are approximately located on a two dimensional grid regularly. SMP technology makes it pos-

sible to analyze the spatial distribution of gene expression, which contributes greatly to studies on gene function and various biological activities (Crosetto et al., 2015).

With the development of SMP techniques, a series of questions worth studying have emerged. One of the most important ones is to identify genes that display spatial expression patterns, which are referred as spatially variable (SV) genes. The study of gene expression spatial heterogeneity could reveal great insights into many aspects, such as embryo development, the cooperation of cellular processes for higher-order biological functions, and the clinical impact of intra-tumor heterogeneity (Bedard et al., 2013; de Bruin et al., 2014). To comprehensively study the diversity of spatial distributions of gene expression, efficient statistical models are urgently needed. There are several existing methods for gene spatial expression analysis: Trendsceek (Edsgård et al., 2018), SpatialDE (Svensson et al., 2018), SPARK (Sun et al., 2020) and BinSpect (Dries, Zhu, Dong, Eng, Li, Liu, Fu, Zhao, Sarkar, Bao, et al., Dries et al.). Trendsceek is based on marked point processes, which has expensive computational cost and unsatisfying performance for SV gene identification (Sun et al., 2020). SpatialDE and SPARK build upon the geostatistical model with Gaussian process, which rely on the selection of pre-defined kernels to account for spatial expression patterns. These two methods are computationally efficient. However, these *ad hoc* kernel functions used for modeling spatial correlation have only specific types, which are not adequate to represent all potential spatial patterns of gene expression. Binspect binarizes normalized gene expression values and summarizes the expressions between neighboring locations via a contingency table, which can be interpreted simply and has extremely low computational cost. However, BinSpect is not a model-based method, indicating that it does not have the

ability to quantify the gene expression spatial dependency. Moreover, the step for creating binary expressions is very sensitive to zero counts and extreme values. If the binarization step is based on setting cutoff on rank, it is also sensitive to the choices of thresholds.

For spatial transcriptomics data, one characteristic is that sample points are approximately located on a two dimensional lattice, which is defined not as a continuous space but a grid. None of the existing approaches take advantage of the discrete space of sample points. In this paper, we proposed a Bayesian model specifically for spatial transcriptomics data, referred as Bayesian mOdeling Of Spatial Transcriptomics data via a modified Ising model (BOOST-Ising). It is a novel Bayesian framework measuring the spatial correlation through potential energy function in the Ising model, which is widely applied on modeling lattice statistics. It consists of three major steps: (1) normalization of the raw gene expression count data; (2) dichotomizing relative expression levels through clustering methods; (3) estimation of spatial correlation via the Ising model with external fields. An auxiliary variable Monte Carlo Markov Chain (MCMC) algorithm is utilized to fit the modified Ising model. One novelty of our method is to model spatial correlation via the Ising model with external fields, which avoids defining specific spatial dependency in advance and results in a more comprehensive SV gene detection. Our method discretizes the normalized count data so that the modeling becomes more robust since the influence of extreme values is eliminated in the clustering step. Unlike BinSpect, outliers and zero counts are considered and excluded in the clustering step. Besides, BOOST-Ising applied a Bayesian framework for SV gene identification to improve quantifying uncertainties and combine prior knowledge into the model. We verified the advantages of BOOST-Ising on simulated data with various

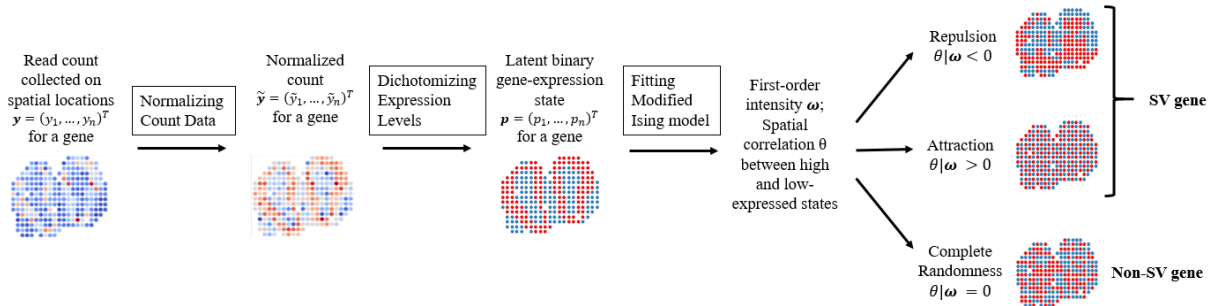


FIG. 1. Schematic of the BOOST-Ising method: θ is the interaction parameter between low-expression and high-expression states in the modified Ising model.

spatial patterns and different zero-inflation setting in the simulation study. Two real spatial transcriptomics datasets were analysed through our method. For both simulation result and real data analysis result, BOOST-Ising exhibited an outstanding performance compared to other existing methods.

The remainder of the paper is arranged as follows. In Section 2, we introduces the BOOST-Ising method including data normalization, data dichotomization and spatial correlation estimation. Section 3 shows the performance of the proposed approach on simulated data. In Section 4, we display the result of BOOST-Ising on two real datasets. Section 5 concludes the article and discusses future research directions.

II. METHODS

In this section, we introduced the method of BOOST-Ising to identify SV genes. A method schematic of BOOST-Ising is shown in Figure 1.

Denote \mathbf{Y} as the $n \times p$ gene expression count matrix generated by SMP technologies. Each entry in matrix $y_{ij} \in \mathbb{N}$ ($i = 1, 2, \dots, n; j = 1, 2, \dots, p$) is the gene expression count

at sample (i.e., location) i for gene j . In total there are p genes and n sample points. Let an $n \times 2$ matrix \mathbf{T} denote the location matrix, where each row \mathbf{t}_i is the sample spatial coordinates (i.e. location information) for sample i ($i = 1, 2, \dots, n$). Since we studied the spatial transcriptomics datasets obtained by sequencing-based SMP techniques, these sample points are approximately located on integer points on a two-dimensional plane. After rounding the spatial coordinates into integers, we had the location matrix \mathbf{T} satisfying each entry $t_{ij} \in \mathbb{N}$. Denote an $n \times p$ matrix \mathbf{P} as the latent indicator matrix. Each entry in matrix $p_{ij} \in \{0, 1\}$ ($i = 1, 2, \dots, n; j = 1, 2, \dots, p$) is the gene expression state indicator at sample (i.e. location) i for gene j . To be specific, $p_{ij} = 0$ indicates the target gene j is low-expressed at location i and $p_{ij} = 1$ indicates it is high-expressed.

A. Normalizing sequencing count data

For the purpose of identifying genes with spatial expression patterns, it is necessary to eliminate the influence of cell size. For instance, if the distribution of relative cell sizes show spatial dependencies, it is hard to distinguish whether the spatial pattern displayed by raw gene expression counts is from cell sizes or gene expression spatial dependencies. Therefore, although there are many instances where variation in cell size itself is of biological interest, we study the regulation of gene expression independent of cell size. We denote s_i as the size factor of sample i , reflecting many nuisance effects including cell size. In our model, we followed a recent spatial transcriptomics study (Sun et al., 2020) directly setting $s_i = Y_i$, which is the summation of the total number of counts across all genes for sample i . Then, the normalized gene expression count $\tilde{y}_{ij} = y_{ij}/s_i$. If the main interest is in the absolute gene

expression level, s_i 's can be set to 1. There are a number of other widely used normalization methods by estimating the cell size factor s_i , such as upper-quartiles (Q75) (Bullard et al., 2010), relative log expression (RLE) (Anders and Huber, 2010), trimmed mean method (TMM) (Robinson and Oshlack, 2010), and so on. Besides, variance stabilizing transformations, such as naive transformation, Anscombe's transformation, followed by regressing out the log scale of total counts, are also commonly applied normalization methods for SMP data. Supplementary Notes lists commonly applied normalization methods for sequencing count data. We conducted a sensitivity analysis for normalization methods, and found that the SV gene identification is robust to the different definition of size factor s_i . For details, see the Supplementary notes.

B. Dichotomizing relative expression levels

After data normalization, we aimed to dichotomize the complex sequencing count data $\tilde{y}_{.j}$ into latent binary gene expression levels for each gene. The reasons for discretizing normalized count data are: (1) to reduce the influence of outliers, resulting in a more robust inference; (2) to process the data into the form that can be fitted by the Ising model. We applied one-dimensional clustering to transform normalized count data into binary expression level indicators for each gene. Here we provided two choices of clustering methods: K-means and Gaussian Mixture Clustering. Unlike BinSpect, when implementing clustering algorithms, we excluded the right tail outliers and zeros in order to obtain a more robust clustering result. To be specific, for each gene, if the normalized count \tilde{y}_{ij} is larger than $\text{median}_j + 3\text{IQR}_j$ (median_j and IQR_j are the median and interquartile range of vector

$\tilde{y}_{.j}$), then we automatically classify this normalized count into high-expression level, while zero counts are directly assigned into low-expression level. Clustering algorithms are only applied to remaining normalized counts for each gene. We conducted a sensitivity analysis for clustering methods, and the results show that the performance of identifying SV genes is robust to the choice of clustering methods. For details, see the Supplementary notes.

1. *Distance-based choice*

K-means (MacQueen et al., 1967) is one of the most commonly used distance-based clustering algorithm. The basic idea of the K-means is to cluster each observation in the cluster with the nearest cluster centroid typically based on Euclidean distance. The main steps of K-means clustering algorithm are firstly to pre-divide the data into k groups, then randomly select k objects as the initial cluster centers. For iteration, calculate the distance between each object and each seed cluster center, and assign each object to the closest distance to it. Each time a sample is allocated, the cluster center of the cluster will be recalculated based on the existing objects in the cluster. This process will continue to repeat until a certain termination condition is met, which can be that no (or less than a minimum number) of objects are reassigned to different clusters. In our study, we applied K-means clustering algorithms for normalized counts for each gene to obtain two clusters. Then binary indicator $p_{.j}$ can be defined as $p_{ij} = 0$ if \tilde{y}_{ij} belongs to the cluster with lower cluster center, and $p_{ij} = 1$ if \tilde{y}_{ij} belongs to the other cluster.

2. *Model-based choice*

A Gaussian mixture clustering (GMC) (Banfield and Raftery, 1993) is a probabilistic model that assumes all the data points are generated from a mixture of a finite number of Gaussian distributions with unknown parameters. Under the gene expression scenario, we assumed that the normalized count was from a mixture of two one-dimensional Gaussian distributions.

$$\begin{aligned} p(\tilde{y}_{ij}) &= \pi_0 p(\tilde{y}_{ij} | p_{ij} = 0) + (1 - \pi_0) p(\tilde{y}_{ij} | p_{ij} = 1) \\ &= \pi_0 \mathcal{N}(\tilde{y}_{ij}; \mu_{0j}, \sigma_{0j}^2) + (1 - \pi_0) \mathcal{N}(\tilde{y}_{ij}; \mu_{1j}, \sigma_{1j}^2) \end{aligned}$$

p_{ij} was the latent binary indicator for the component that \tilde{y}_{ij} belonged to. We implemented the expectation-maximization (EM) algorithm to fit GMC using R package 'mclust' (Scrucca et al., 2016) for each gene and the estimated p_{ij} 's were directly the binary expression level indicators we wanted. Note that if the estimated μ_{0j} is larger than μ_{1j} , we need to switch p_{ij} to $1 - p_{ij}$ so that indicators are consistent with the definition that $p_{ij} = 0$ means \tilde{y}_{ij} belongs to low-expression level.

C. Identifying SV genes via a modified Ising model

1. *A brief review of the Ising model*

In statistical mechanics, the Ising model, a special case of the Potts model (Wu, 1982), is a model of interacting spins on a crystalline lattice (Cipra, 1987). In statistics, we consider the Ising model as an undirected graph such that each vertex is geometrically regular assigned

on a lattice and each edge is of the same length. Each vertex has one of two states. In the context of spatial transcriptomics, vertices refer to array spots on a square lattice system, where each spot at location $t_i = (t_{i1}, t_{i2})$ has up to four neighbors at locations $(t_{i1} + 1, t_{i2})$, $(t_{i1} - 1, t_{i2})$, $(t_{i1}, t_{i2} + 1)$, and $(t_{i1}, t_{i2} - 1)$ if applicable. For a gene of interest, each spot will be assigned with a binary state p_i , representing the expression level at location t_i . Hamiltonian, the energy measurement of all spins, for classic Ising model is:

$$H(\mathbf{p}|\theta) = - \sum_{i \sim i'} \theta I_0(p_i \neq p_{i'}),$$

where $i \sim i'$ denotes the collection of all neighboring spot pairs, I_0 is the indicator function and θ is the interaction parameter between two states. In this energy measurement, only those edges between spins that have different states are counted. According to the fundamental Hammersley-Clifford theorem (Clifford, 1990), if we have a locally defined energy such as Hamiltonian, then a probability measure with a Markov property exists:

$$\Pr(\mathbf{p}|\theta) = \frac{\exp(-H(\mathbf{p}|\theta))}{\sum_{\mathbf{p}'} \exp(-H(\mathbf{p}'|\theta))}$$

In this model, θ is the parameter quantifying the spatial correlation between adjacent points, which is also called as the second-order intensity parameter. Suppose there are only two adjacent points on the lattice, we can easily derive the conditional probability of one point p_1 given the state of the other point $p_2 = q$ as

$$\Pr(p_1 = q' | p_2 = q, \theta) = \frac{\exp(\theta)}{1 + \exp(\theta)}, \quad q' \neq q$$

where q' and q represent two states in the Ising model. $\Pr(p_1 = q'|p_2 = q, \theta) > 0.5$ if $\theta > 0$ and the larger the value of θ is, the higher probability that two points have different states. If $\theta = 0$, $\Pr(p_1 = q'|p_2 = q, \theta) = \Pr(p_1 = q') = 0.5$, indicating that there is no spatial correlation between points. For negative θ , points with same states tend to gather, since the conditional probability of p_1 having the same state as p_2 , i.e., $\Pr(p_1 = q|p_2 = q, \theta)$ is greater than 0.5 if $\theta < 0$. The probability that two points has same states increases with the decrease of θ . The above instance illustrates that the spatial correlations among points can be easily interpreted by the value of interaction parameter θ .

2. *Modified Ising model with first-order intensity parameters*

Under the gene expression level scenario, the proportion of two states are imbalanced, indicating that the classic Ising model is no longer suitable. Therefore, we modified the Ising model by adding a first-order intensity parameter $\boldsymbol{\omega} = (\omega_0, \omega_1)$, which represents the proportion of each state. In mechanics, $\boldsymbol{\omega}$ corresponds to the presence of an external magnetic field. After modification, the Hamiltonian energy measurement is

$$H(\mathbf{p}|\theta, \boldsymbol{\omega}) = - \sum_i \omega_{p_i} - \sum_{i \sim i'} \theta I_0(p_i \neq p_{i'}),$$

The modified Ising model probability mass function calculates the probability of observing the lattice in a particular configuration \mathbf{p} :

$$\begin{aligned}
\Pr(\mathbf{p}|\theta, \boldsymbol{\omega}) &= \frac{\exp(-H(\mathbf{p}|\theta, \boldsymbol{\omega}))}{\sum_{\mathbf{p}'} \exp(-H(\mathbf{p}'|\theta, \boldsymbol{\omega}))} \\
&= \frac{1}{C(\theta, \boldsymbol{\omega})} \exp(-H(\mathbf{p}|\theta, \boldsymbol{\omega})) \\
&= \frac{1}{C(\theta, \boldsymbol{\omega})} \exp(-(\sum_i -\omega_{p_i} - \sum_{i \sim i'} \theta I_0(p_i \neq p_{i'}))),
\end{aligned} \tag{1}$$

where the denominator $C(\theta, \boldsymbol{\omega})$ is the normalizing constant that needs to sum over the entire space of \mathbf{p}' , consisting of 2^n configurations. The meaning of parameters θ and $\boldsymbol{\omega}$ can be interpreted through the probability measurement. Firstly, the probability expression reduces to $\Pr(p = i) \propto \exp(\omega_i)$, $i = 0, 1$ if there is only one point on the lattice, which implies the probability of observing a point with state i in this single-point system is equal to $\pi_i = \frac{\exp(\omega_i)}{\exp(\omega_0) + \exp(\omega_1)}$. From the example, we can see that parameter $\boldsymbol{\omega}$ describes the proportion of different states. Parameter θ indicates the spatial correlations between states in the Ising model, which is our primary interest. Same as in the classical Ising model, the probability measurement reveals that the smaller the value of $\theta < 0$, the more likely that spot i 's state is concordant with the majority of its neighbors' states, thereby exhibiting a spatial expression pattern across all locations. If $\theta = 0$, then each spot has an equivalent probability of belonging to either state, resulting in complete spatial randomness. If $\theta > 0$, there exists attraction between two states. The right side of Figure 1 shows the relationship between the interaction parameter θ and the spatial distribution of spins \mathbf{p} . We defined genes having negative interaction parameter θ as SV genes. However, if a gene has a positive

interaction parameter, there is a special spatial dependency between high-expression level and low-expression level, which is also referred to an SV gene and worth further exploration.

3. *Model fitting via double Metropolis-Hastings algorithm*

We applied MCMC algorithms to fit the modified Ising model. However, the standard Metropolis-Hastings (MH) algorithm cannot be directly applied to simulate from a distribution with intractable normalizing constant $C(\theta, \omega)$. To address this issue, we used an auxiliary variable MCMC algorithm, known as double Metropolis-Hastings (DMH) algorithm (Liang, 2010; Liang et al., 2016), which is able to make the normalizing constant ratio canceled by augmenting appropriate auxiliary variables through a short run of the MH algorithm initialized with the original observation. The detailed introduction of MCMC algorithms is in Supplementary Notes.

Our primary interest lied in the identification of SV genes via the interaction parameter θ . Here we aimed to make inference for the hypothesis testing $\mathcal{M}_0 : \theta \geq 0$ versus $\mathcal{M}_1 : \theta < 0$. If there was strong evidence to reject the null hypotheses \mathcal{M}_0 , we concluded that the gene was an SV gene.

A comprehensive summary of θ is to select the SV gene based on the Bayes factor. We calculated the Bayes factor measuring the favor of \mathcal{M}_1 as

$$\text{BF}^j = \frac{\Pr(\mathbf{p}_{\cdot j} | \mathcal{M}_1)}{\Pr(\mathbf{p}_{\cdot j} | \mathcal{M}_0)} = \frac{\Pr(\mathcal{M}_1 | \mathbf{p}_{\cdot j}) \Pr(\mathcal{M}_0)}{\Pr(\mathcal{M}_0 | \mathbf{p}_{\cdot j}) \Pr(\mathcal{M}_1)},$$

where $\mathbf{p}_{\cdot j}$ is the binary indicator for gene j . From the prior distribution of θ , we have that $\Pr(\mathcal{M}_0) = \Pr(\mathcal{M}_1) = 0.5$, so

$$\text{BF}^j = \frac{\Pr(\mathcal{M}_1|\mathbf{p}_{\cdot j})}{\Pr(\mathcal{M}_0|\mathbf{p}_{\cdot j})} = \frac{\sum_{u=1}^U I(\theta_j^{(u)} < 0)}{\sum_{u=1}^U I(\theta_j^{(u)} \geq 0)}$$

For inference, we can choose the threshold based on the scale for interpretation of Bayes factor proposed by (Kass and Raftery, 1995).

To detect SV genes having spatial pattern with the positive interaction parameter, we used the Bayes factor BF^j measuring the favor of \mathcal{M}_0 against \mathcal{M}_1 and did inference via the same thresholds.

III. SIMULATION STUDY

We performed a series of simulations to evaluate the performance of BOOST-Ising and compared it with four existing methods: SPARK, SpatialDE, BinSpect-km and BinSpect-rank. BinSpect-km applies k-means to binarize expression counts and BinSpect-rank is based on setting cutoff on rank to obtain binary expressions. We generated the simulated gene expression data based on the data generating process in Sun et al. 2020, Li et al. 2020 and Edsgård et al. 2018. Five methods, i.e., BOOST-Ising and other four existing methods, were evaluated for the ability to identify SV genes displaying five distinct spatial patterns, including two artificially generated spatial patterns (Figure 2(a) and (b)), two real spatial patterns in mouse olfactory bulb (MOB) and human breast cancer (BC) data respectively (Figure 2(c) and (e)), and one special spatial pattern corresponding with positive interaction parameter in the Ising model (Figure 2(d)). In the MOB and BC datasets,

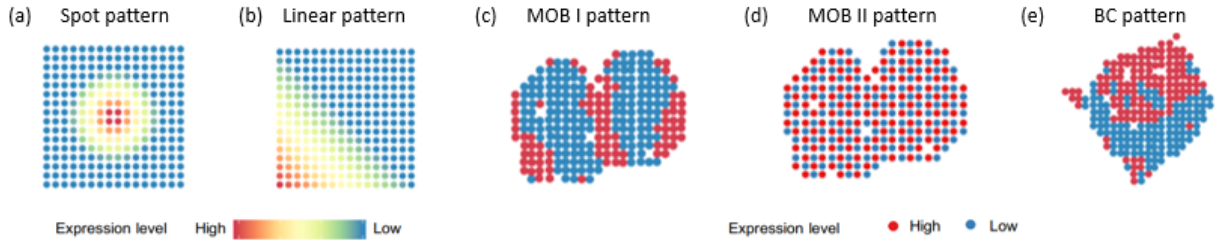


FIG. 2. Spatial patterns applied in the simulation study: (a) and (b) are artificially generated patterns; (c) and (e) are binary patterns that were summarized based on SV genes detected by SPARK in MOB data and BC data, respectively; (d) is the spatial pattern generated by the Ising model with positive interaction parameter θ .

over 90% of genes have a proportion of zero expression counts greater than 10%. In the BC dataset, especially, there are still 83.6% of genes with a proportion of zero expression counts greater than 50% after excluding genes having proportion of zero counts greater than 80%. Therefore, we applied zero-inflation when generating simulated data in order to better reflect the circumstance in real datasets. The detailed simulated spatial patterns and data generating process is illustrated in the Supplementary Notes. We set three choices of zero-inflated rate π_i , 10%, 30% and 50%. To summarize, we had in total 15 scenarios, which were the combinations of three zero-inflated choices and five potential spatial patterns. In each scenario, 10 datasets were generated independently for the performance estimation.

We chose GMC as the clustering technique for dichotomizing relative gene expression levels in BOOST-Ising. For prior specification in the MCMC algorithms of Ising model fitting, we recommended the settings of hyperparameters as the standard deviation of prior for interaction parameter $\sigma_\theta = 1/3$ and for first-order intensity parameter $\sigma_\omega = 2.5$, which is thoroughly discussed in the Supplementary notes. For the BOOST-Ising algorithm, we ran four independent MCMC chains with 10,000 iterations in each chain, excluding the first half

iterations as burn-in. Initial values of all parameters for each chain were randomly drawn from their prior distribution. Results in the following analysis were obtained by pooling the MCMC outputs from the four chains together. To check whether the obtained posterior samples converge, we used the potential scale reduction factor (PSRF) to evaluate convergence. PSRFs under all scenarios for all genes were less than 1.1, indicating the convergence of MCMC algorithms in the simulation study. All experiments were implemented in R with Rcpp package to accelerate computations.

We treated the detection of SV genes as a binary classification problem and evaluated the performance of our method and the other two approaches through commonly applied criteria for binary classifiers. In binary classification problems, the outcome of a classifier can be summarized into four categories: true positive (TP), false positive (FP), false negative (FN) and true negative (TN). The first criterion we applied is the area under the receiver operating characteristic (ROC) curve (AUC). The ROC curve is based on a series of different cut-off values or decision thresholds, with TP rate as the vertical coordinate and FP rate as the x coordinate. The AUC is a relatively comprehensive performance measure for binary classifier. AUC has range from 0 to 1 and higher score means better performance. Another measure of performance applied is Matthews correlation coefficient (MCC) ([Matthews, 1975](#)), which is widely used for evaluation of imbalanced classification outcomes. MCC is defined as

$$\text{MCC} = \frac{(\text{TP} \times \text{TN} - \text{FP} \times \text{FN})}{\sqrt{(\text{TP} + \text{FP})(\text{TP} + \text{FN})(\text{TN} + \text{FP})(\text{TN} + \text{FN})}}$$

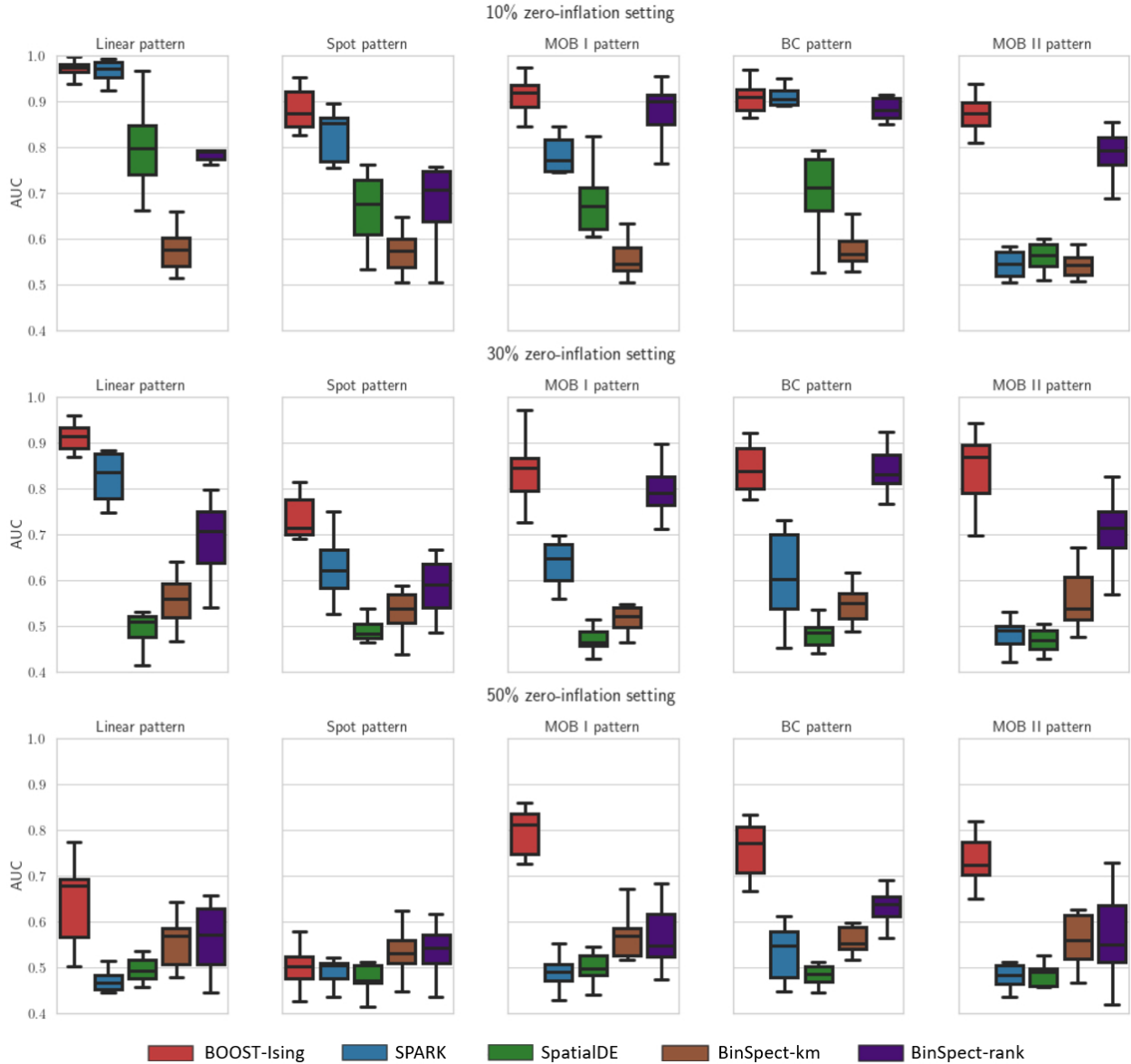


FIG. 3. Boxplots of AUCs measuring the performance of identifying SV genes by BOOST-Ising, SPARK, SpatialDE, BinSpect-km and BinSpect-rank under different scenarios

It combines together four types of outcomes, TP, FP, FN and TN and provides an informative single score to qualify a binary classifier. MCC has range from -1 to 1, where a value of 1 means 100% accurate, and a value less than 0 means the classifier is even worse than totally random classification.

Figure 3 displays the boxplots of AUCs obtained by applying three approaches on 10 replicated datasets under different scenarios. Firstly, we can see that neither SPARK nor SpatialDE had the ability to detect SV genes with the MOB II pattern, which was the pattern generated from the Ising model with positive interaction parameter. It is not surprising since the MOB II pattern is not included by the pre-defined kernel functions in SPARK and SpatialDE. However, BOOST-Ising showed satisfactory results on detecting MOB II pattern under all three zero-inflation settings. BinSpect-rank could detect SV genes with the MOB II pattern, but the performance was not so good as BOOST-Ising. In terms of low zero-inflation setting, SPARK and BOOST-Ising had similar performance on detecting SV genes with linear and BC pattern, and BOOST-Ising had obvious superiority when identifying SV genes with spot and MOB I pattern. BinSpect-rank and BOOST-Ising were similar for binary patterns, while BinSpect-rank had poor performance on continuous patterns, i.e., linear and spot patterns. SpatialDE and BinSpect-km performed worse than our approach in the all five spatial patterns and all zero-inflation settings, indicating that these two methods are very sensitive to even low zero-inflation situation. Under the medium or high zero inflation, BOOST-Ising was much more powerful than the other methods. Specifically, SPARK and SpatialDE completely lost their power under high zero-inflation setting, while BOOST-Ising still had almost uninfluenced performance. Although we did not model zero-inflation in BOOST-Ising, dichotomizing relative expression rates did eliminate the influence of zero counts. BinSpect-rank could handle zero-inflation issues for binary patterns, but sharp decrease in AUCs under high zero-inflation setting showed that it is not robust to variance brought by high proportion of zero counts. For spot pattern under high zero-

inflation setting, BOOST-Ising had poor performance, which is not surprising since high zero proportion may seriously disturb the spot pattern and lead to generated SV genes having no obvious spatial patterns.

To calculate MCC, we need to set cutoff of SV gene selection for three different methods. For other methods, we set the significance level of detecting SV genes as 0.05. To control the type I error rate, we directly applied the p-value adjustment strategies included in their papers. For BOOST-Ising, we selected a gene as an SV gene if it had very strong evidence against the null hypotheses, i.e. Bayes factor is greater than 150. Table I shows results of average MCCs by three methods over 10 replicated datasets under each setting. Similar to what was showed by the AUCs, BOOST-Ising had outstanding performance compared with other methods, especially under medium and high zero-inflation settings. MCCs for BinSpect-rank under medium and high zero-inflation are higher than other three existing methods, but are still lower than our approach for majority of patterns. MCCs for SpatialDE under medium and high zero-inflation and for SPARK and high zero-inflation shows their failures to detect SV genes. Although MCCs decreased for BOOST-Ising, it still had the power to select SV genes with a high proportion of zero counts under almost simulated patterns.

IV. REAL DATA ANALYSIS

We applied the BOOST-Ising method to analyze two published datasets obtained by spatial transcriptomics sequencing, the mouse olfactory bulb (MOB) and human breast

TABLE I. Averaged MCCs (standard deviations) by BOOST-Ising, SPARK, SpatialDE, BinSpect-km and BinSpect-rank under different scenarios

10% zero inflation setting					
	Spot	Linear	MOB I	BC	MOB II
BOOST-Ising	0.519(0.071)	0.853 (0.054)	0.626(0.086)	0.531(0.108)	0.642 (0.103)
SPARK	0.624 (0.091)	0.768(0.053)	0.488(0.116)	0.652 (0.083)	0.000(0.000)
SpatialDE	0.128(0.136)	0.497(0.102)	0.184(0.203)	0.276(0.197)	0.000(0.000)
BinSpect-km	0.061(0.117)	0.036(0.102)	-0.019(0.035)	-0.021(0.032)	0.041(0.158)
BinSpect-rank	0.341(0.176)	0.418(0.167)	0.632 (0.080)	0.639(0.111)	0.333(0.172)
30% zero inflation setting					
	Spot	Linear	MOB I	BC	MOB II
BOOST-Ising	0.237 (0.155)	0.604 (0.077)	0.501 (0.157)	0.398(0.071)	0.568 (0.095)
SPARK	0.055(0.048)	0.342(0.164)	0.065(0.113)	0.058(0.124)	0.000(0.000)
SpatialDE	0.000(0.000)	0.000(0.000)	0.000(0.000)	0.000(0.000)	0.000(0.000)
BinSpect-km	0.049(0.126)	-0.004(0.076)	-0.027(0.098)	-0.031(0.030)	0.010(0.065)
BinSpect-rank	0.067(0.111)	0.242(0.055)	0.478(0.139)	0.567 (0.112)	0.306(0.096)
50% zero inflation setting					
	Spot	Linear	MOB I	BC	MOB II
BOOST-Ising	0.046 (0.108)	0.175 (0.158)	0.368 (0.107)	0.288 (0.139)	0.249 (0.166)
SPARK	0.000(0.000)	0.024(0.076)	0.000(0.000)	0.048(0.101)	0.000(0.000)
SpatialDE	0.000(0.000)	0.000(0.000)	0.000(0.000)	0.000(0.000)	0.000(0.000)
BinSpect-km	0.046 (0.089)	0.008(0.108)	0.018(0.078)	-0.044(0.063)	0.024(0.096)
BinSpect-rank	0.046 (0.122)	0.075(0.141)	0.095(0.097)	0.197(0.102)	0.021(0.100)

cancer 21 (BC) data. Before detecting SV genes, filtration for the data was conducted to remove non-informative genes and spots. To be specific, we excluded: (1) spots with fewer than ten total counts across all genes; (2) genes that were not expressed in over 80% of

locations. We chose GMC as our clustering method to dichotomize normalized expression counts. In MCMC algorithms of BOOST-Ising, we set the same hyperparameters as in the simulation study. We selected genes as SV genes if they had very strong evidence against null hypotheses, i.e. Bayes factor is greater than 150. For SPARK and SpatialDE, we applied the filtration strategies and selection criteria exactly as proposed in their papers.

A. Mouse olfactory bulb dataset

The MOB dataset is a study on mouse olfactory bulb through spatial transcriptomic sequencing technique, which can be downloaded from Spatial Research (<http://www.spatialresearch.org>). There are 12 replicates. Each one has 15,284 to 16,675 genes measured on 231 - 282 spots. Following the SPARK and SpatialDE paper, ‘MOB Replicate 11’ file was analyzed for MOB dataset, containing 16,218 genes with 262 sample points.

After filtering, there were a total of 9,769 genes and 260 spots in MOB dataset. BOOST-Ising identified 734 SV genes, which was approximately the same number of SV genes detected by SPARK and around ten times the number of SV genes detected by SpatialDE. Figure 4(a) is the Venn diagram showing the overlap of detected SV genes by SpatialDE, SPARK and our methods. BOOST-Ising detected a lot of SV genes in common with the other two methods, while there were also many uniquely SV genes identified only by BOOST-Ising or SPARK. Most of the SV genes detected by SpatialDE were also included in the result of SPARK or BOOST-Ising, which indicates that SpatialDE is a relatively conservative method for SV gene identification.

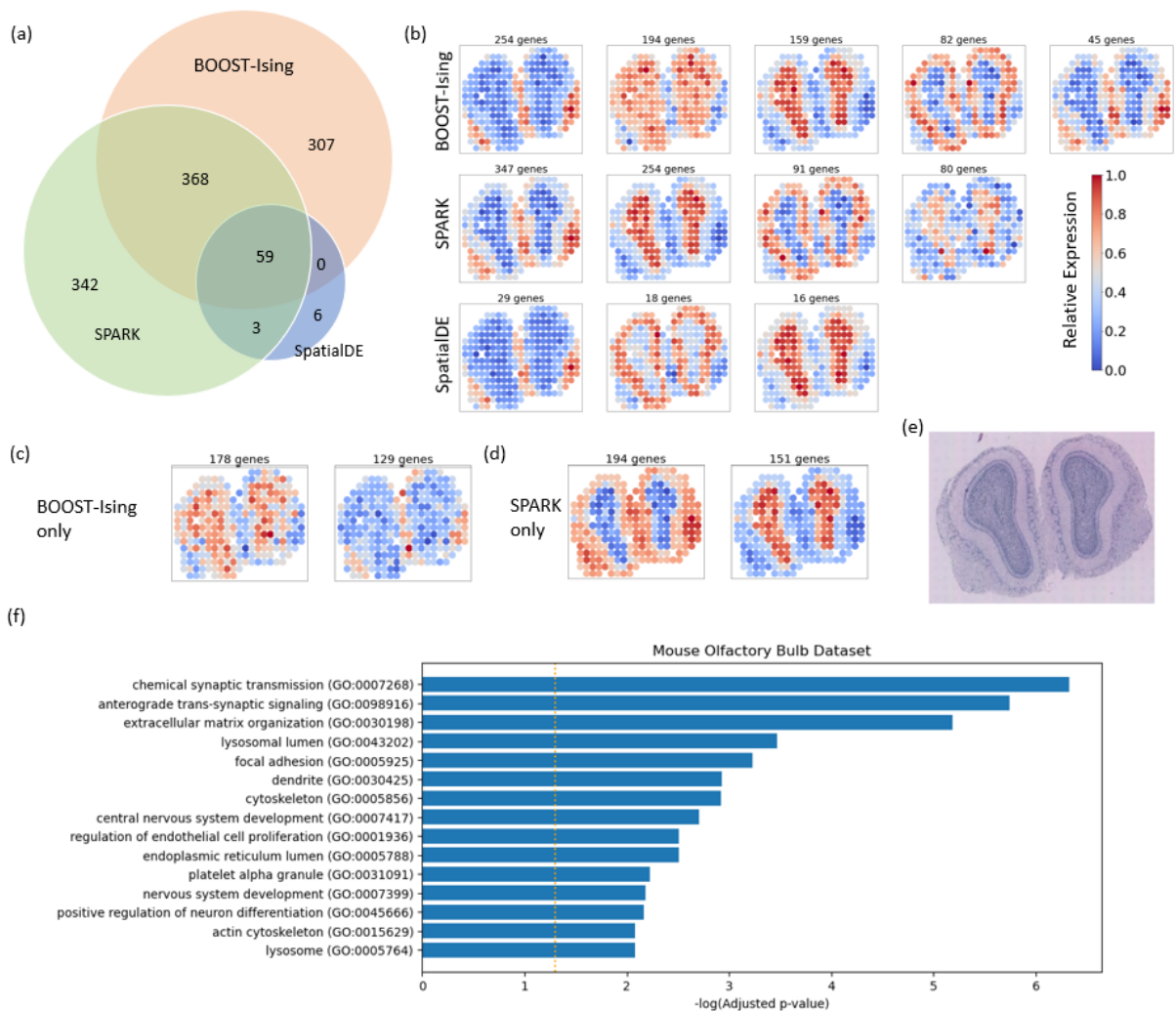


FIG. 4. Analysis result of the MOB dataset: (a) Venn diagram showing the overlap among SV genes identified by BOOST-Ising, SPARK and SpatialDE; (b) Distinct spatial expression patterns of SV genes identified by BOOST-Ising, SPARK and SpatialDE; (c) Spatial expression patterns of SV genes identified by BOOST-Ising only; (d) Spatial expression patterns of SV genes identified by SPARK only; (e) The associated hematoxylin and eosin (H&E)-stained tissue slides of MOB data; (f) Gene ontology (GO) enrichment analysis of SV genes identified by BOOST-Ising in MOB data. Orange dashed line indicates a significance level of 0.05.

In order to further explore types of patterns we had found through each method, we did the agglomerative hierarchical clustering on the SV genes identified by each of three methods. Before clustering, we firstly applied the normalization method proposed in [Svensson et al.](#)

2018 to deal with raw counts. The number of clusters was determined by cutting the hierarchical clustering dendrogram at a height reflecting a clear cluster separation. To visualize the clustering result, we summarized the expression patterns via the averaged expression levels within each cluster. SV genes detected by BOOST-Ising were clustered into five groups, while there were four groups for SPARK and three clusters for SpatialDE, shown in Figure 4(b). Consistent with results reported by Sun et al. 2020, there were three major gene expression patterns which could be detected by all three methods. However, a unique pattern (the second pattern in BOOST-Ising in Figure 4(b)) could only be detected by BOOST-Ising with 194 SV genes, which indicates the superiority of our method. To compare results between SPARK and our method, we did clustering on the SV genes only detected by SPARK or by BOOST-Ising, which is shown in Figure 4(c) and (d). 307 genes identified only by BOOST-Ising could be mainly categorized to two patterns, including the unique pattern with 178 genes. SV genes only detected by SPARK showed strong periodic pattern, suggesting that SPARK might be more sensitive to smooth periodic spatial pattern.

Finally, we performed gene ontology (GO) enrichment analysis of SV genes identified by BOOST-Ising to explore relevant biological functions of these SV genes. A total of 3,929 mouse GO terms in three components (biological processes, cellular components and molecular functions) had at least one gene overlap with detected SV gene via BOOST-Ising. Controlling the false discovery rate at 0.05, 155 GO terms were found in MOB dataset. 15 GO terms with the smallest p-values are shown in Figure 4(f). As with SPARK, many enriched gene sets for SV genes detected by BOOST-Ising are related to synaptic

signaling and nervous system, which made significant contributions in synaptic organization and olfactory bulb development.

In the MOB dataset, 60 genes were detected to have spatial pattern with positive interaction parameter through BOOST-Ising. Table 2 in Supplementary Notes lists all detected SV genes with positive interaction parameter. To analyze the potential biological functions of these SV genes, we performed functional enrichment analysis. 603 mouse GO terms and 43 Kyoto Encyclopedia of Genes and Genomes (KEGG) terms had at least one gene overlap with these SV genes. We also found some statistically significant GO and KEGG terms, which had adjusted p-values less than 0.05. For instance, holo TFIIH complex (GO:0005675) and nucleotide excision repair KEGG term were significantly enriched (adjusted p-value 0.040 and 0.013 respectively) in the detected SV genes with positive interaction parameter by BOOST-Ising. Thus, the discovery above highlights the advantage of implementing gene spatial expression analysis with BOOST-Ising.

B. Human breast cancer dataset

The BC dataset was from human breast cancer biopsies obtained by spatial transcriptomic sequencing technique. Four layers were included in this dataset. Each one had around 15,000 genes sampled on 251 to 264 spots. Following implementation of other SV gene detection methods, we applied ‘Breast Cancer Layer 2’ for BC dataset, containing 14,789 genes measured on 251 spots.

After filtration, 2,280 genes and 250 spots were included in the BC dataset. There were 302 SV genes identified by BOOST-Ising, which was slightly larger than the number of SV

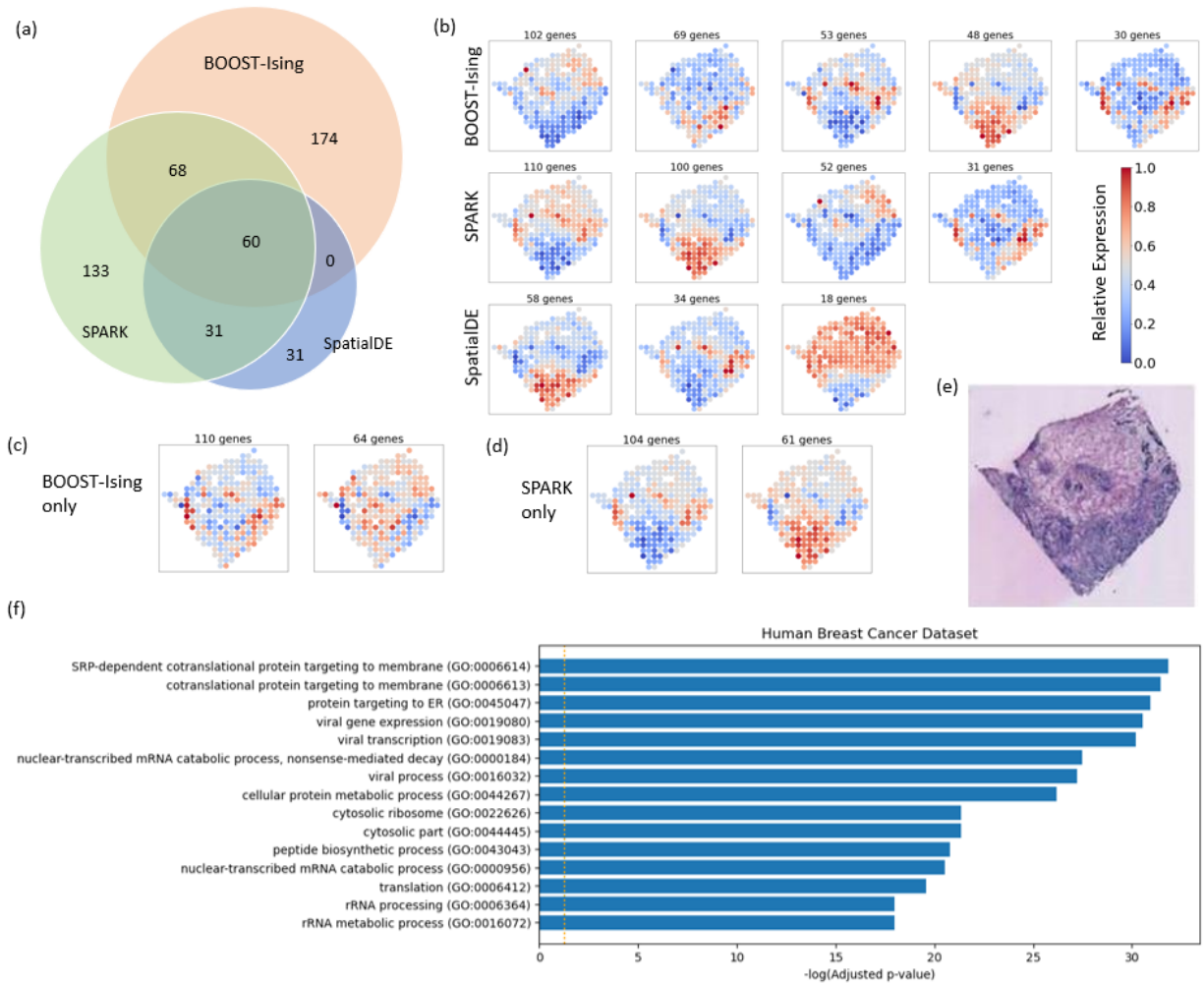


FIG. 5. Analysis result of the BC dataset: (a) Venn diagram showing the overlap among SV genes identified by BOOST-Ising, SPARK and SpatialDE; (b) Distinct spatial expression patterns of SV genes identified by BOOST-Ising, SPARK and SpatialDE; (c) Spatial expression patterns of SV genes identified by BOOST-Ising only; (d) Spatial expression patterns of SV genes identified by SPARK only; (e) The associated hematoxylin and eosin (H&E)-stained tissue slides of BC data; (f) Gene ontology (GO) enrichment analysis of SV genes identified by BOOST-Ising in BC data. Orange dashed line indicates a significance level of 0.05.

genes detected by SPARK and around three times the number of SV genes detected by SpatialDE. A Venn diagram (Figure 5(a)) shows that less than half of SV genes detected by

BOOST-Ising were also included in the result of one of the other two methods. There were also 174 SV genes identified only by BOOST-Ising.

Following the same hierarchical clustering strategies in MOB data, Figure 5(b) shows the expression patterns detected by BOOST-Ising, SPARK and SpatialDE. Five, four and three clusters were obtained for SV genes identified by BOOST-Ising, SPARK and SpatialDE, respectively. All four patterns discovered by SPARK could also be detected by BOOST-Ising. For some of the four patterns, BOOST-Ising detected more SV genes than SPARK. For example, our method detected 102 genes with the first pattern for BOOST-Ising in Figure 5(b), while SPARK detected 52 SV genes with this pattern. However, for some patterns, BOOST-Ising identified fewer SV genes than SPARK. The second pattern for BOOST-Ising is a unique pattern that could only be detected by BOOST-Ising, which is approximately the complement pattern with the first pattern for BOOST-Ising. To clearly compare results between SPARK and our method, we did clustering on the SV genes only detected by SPARK or by BOOST-Ising, which is shown in Figure 5(c) and (d). Obvious spatial patterns existed for SV genes identified by SPARK or BOOST-Ising only, suggesting that both methods need some improvements to identify SV genes more comprehensively.

Finally, we implemented GO enrichment analysis the same as in the previous MOB data analysis. A total of 2,477 human GO terms had at least one gene overlap with identified SV gene via BOOST-Ising. At an FDR of 5%, 116 GO terms were found in BC dataset. Figure 5(f) shows 15 GO terms with the smallest adjusted p-values. SPARK discovered many enriched gene sets which were related to extracellular matrix organization and immune responses. Although these GO terms were not shown in Figure 5(f), BOOST-Ising did detect

the same related terms with significant result (e.g. the adjusted p-value for extracellular matrix organization (GO:0030198) was 1.53×10^{-14}). Furthermore, more virus-related GO terms were found to be significant in our analysis. There is strong evidence that many types of virus may have association with the causation of human breast cancers ([Lawson and Heng, 2010](#)). For instance, virus life cycle GO term (GO:0019058) was significantly enriched in the detected SV genes by BOOST-Ising, while not statistically significant for SV genes identified by SPARK (the adjusted p-value was 0.829).

V. CONCLUSION

In this paper, we focused on modeling spatial transcriptomics data via a modified Ising model. This Bayesian framework was proposed in order to achieve two goals: (1) to discretize the sequencing count data to result in a more robust inference; and (2) to quantify the spatial correlation between different gene expression levels. Compared to other approaches, BOOST-Ising shows its superiority on several aspects. First, it discretize gene expression counts so that more robust inference can be obtained. More importantly, it models the spatial dependency via the energy measurement and identifies SV genes via quantifying the spatial correlation parameter in the Ising model. In simulation studies, BOOST-Ising had similar power compared with other methods in low zero inflation settings, while had strong ability to deal with excess of zero count problem. In real data, SV genes detected by BOOST-Ising displayed novel spatial patterns and consequential enriched pathways.

Several extensions of our model are worth investigating. First, the proposed model can be extended to model k discrete gene expression levels via the modified Potts model and the

number of components k can be considered as unfixed (Green and Richardson, 2002), so that the count data structure can be captured more thoroughly. Second, a hierarchical Bayesian framework can be developed to directly model the sequencing count data via proper finite mixture distributions and model the latent expression level indicators via the modified Potts model. Moreover, since our approach is limited on lattice sample points, which can only be applied on spatial transcriptomics data, it is necessary to generalize our model feasible for detecting SV genes on data obtained from image-based SMP techniques, such as smFISH data. Finally, it is possible to investigate other approximate Bayesian computation methods to reduce the computational cost of BOOST-Ising. These future directions will improve the performance of BOOST-Ising further.

ACKNOWLEDGEMENTS

Computational support was generously provided by Southern Methodist University's Center for Research Computing. Thanks Jessie Norris for helping us in proofreading the manuscript.

REFERENCE

- Anders, S. and W. Huber (2010). Differential expression analysis for sequence count data. *Nature Precedings*, 1–1.
- Anscombe, F. J. (1948). The transformation of poisson, binomial and negative-binomial data. *Biometrika* 35(3/4), 246–254.
- Banfield, J. D. and A. E. Raftery (1993). Model-based gaussian and non-gaussian clustering. *Biometrics*, 803–821.
- Bedard, P. L., A. R. Hansen, M. J. Ratain, and L. L. Siu (2013). Tumour heterogeneity in the clinic. *Nature* 501(7467), 355–364.
- Bullard, J. H., E. Purdom, K. D. Hansen, and S. Dudoit (2010). Evaluation of statistical methods for normalization and differential expression in mrna-seq experiments. *BMC bioinformatics* 11(1), 1–13.
- Chen, K. H., A. N. Boettiger, J. R. Moffitt, S. Wang, and X. Zhuang (2015). Spatially resolved, highly multiplexed rna profiling in single cells. *Science* 348(6233).
- Cipra, B. A. (1987). An introduction to the ising model. *The American Mathematical Monthly* 94(10), 937–959.
- Clifford, P. (1990). Markov random fields in statistics. *Disorder in physical systems: A volume in honour of John M. Hammersley*, 19–32.
- Crosetto, N., M. Bienko, and A. Van Oudenaarden (2015). Spatially resolved transcriptomics and beyond. *Nature Reviews Genetics* 16(1), 57–66.

- de Bruin, E. C., N. McGranahan, R. Mitter, M. Salm, D. C. Wedge, L. Yates, M. Jamal-Hanjani, S. Shafi, N. Murugaesu, A. J. Rowan, et al. (2014). Spatial and temporal diversity in genomic instability processes defines lung cancer evolution. *Science* 346(6206), 251–256.
- Dries, R., Q. Zhu, R. Dong, C.-H. L. Eng, H. Li, K. Liu, Y. Fu, T. Zhao, A. Sarkar, F. Bao, et al. Giotto, a toolbox for integrative analysis and visualization of spatial expression data. *22*(78).
- Edsgård, D., P. Johnsson, and R. Sandberg (2018). Identification of spatial expression trends in single-cell gene expression data. *Nature methods* 15(5), 339–342.
- Femino, A. M., F. S. Fay, K. Fogarty, and R. H. Singer (1998). Visualization of single rna transcripts in situ. *Science* 280(5363), 585–590.
- Green, P. J. and S. Richardson (2002). Hidden markov models and disease mapping. *Journal of the American statistical association* 97(460), 1055–1070.
- Kass, R. E. and A. E. Raftery (1995). Bayes factors. *Journal of the american statistical association* 90(430), 773–795.
- Lawson, J. S. and B. Heng (2010). Viruses and breast cancer. *Cancers* 2(2), 752–772.
- Li, Q., M. Zhang, Y. Xie, and G. Xiao (2020). Bayesian modeling of spatial molecular profiling data via gaussian process. *arXiv preprint arXiv:2012.03326*.
- Liang, F. (2010). A double metropolis–hastings sampler for spatial models with intractable normalizing constants. *Journal of Statistical Computation and Simulation* 80(9), 1007–1022.
- Liang, F., I. H. Jin, Q. Song, and J. S. Liu (2016). An adaptive exchange algorithm for sampling from distributions with intractable normalizing constants. *Journal of the American*

- Statistical Association* 111(513), 377–393.
- Love, M. I., W. Huber, and S. Anders (2014). Moderated estimation of fold change and dispersion for rna-seq data with *deseq2*. *Genome biology* 15(12), 1–21.
- Lubeck, E., A. F. Coskun, T. Zhiyentayev, M. Ahmad, and L. Cai (2014). Single-cell in situ rna profiling by sequential hybridization. *Nature methods* 11(4), 360.
- MacQueen, J. et al. (1967). Some methods for classification and analysis of multivariate observations. In *Proceedings of the fifth Berkeley symposium on mathematical statistics and probability*, Volume 1, pp. 281–297. Oakland, CA, USA.
- Matthews, B. W. (1975). Comparison of the predicted and observed secondary structure of t4 phage lysozyme. *Biochimica et Biophysica Acta (BBA)-Protein Structure* 405(2), 442–451.
- Robinson, M. D. and A. Oshlack (2010). A scaling normalization method for differential expression analysis of rna-seq data. *Genome biology* 11(3), 1–9.
- Scrucca, L., M. Fop, T. B. Murphy, and A. E. Raftery (2016). *mclust* 5: clustering, classification and density estimation using gaussian finite mixture models. *The R journal* 8(1), 289.
- Shah, S., Y. Takei, W. Zhou, E. Lubeck, J. Yun, C.-H. L. Eng, N. Koulena, C. Cronin, C. Karp, E. J. Liaw, et al. (2018). Dynamics and spatial genomics of the nascent transcriptome by intron seqfish. *Cell* 174(2), 363–376.
- Ståhl, P. L., F. Salmén, S. Vickovic, A. Lundmark, J. F. Navarro, J. Magnusson, S. Giacomello, M. Asp, J. O. Westholm, M. Huss, et al. (2016). Visualization and analysis of gene expression in tissue sections by spatial transcriptomics. *Science* 353(6294), 78–82.

- Sun, S., J. Zhu, and X. Zhou (2020). Statistical analysis of spatial expression patterns for spatially resolved transcriptomic studies. *Nature methods* 17(2), 193–200.
- Svensson, V., S. A. Teichmann, and O. Stegle (2018). Spatialde: identification of spatially variable genes. *Nature methods* 15(5), 343–346.
- Vickovic, S., G. Eraslan, F. Salmén, J. Klughammer, L. Stenbeck, D. Schapiro, T. Äijö, R. Bonneau, L. Bergenstråhle, J. F. Navarro, et al. (2019). High-definition spatial transcriptomics for in situ tissue profiling. *Nature methods* 16(10), 987–990.
- Wu, F.-Y. (1982). The potts model. *Reviews of modern physics* 54(1), 235.
- Zhang, M., T. Sheffield, X. Zhan, Q. Li, D. M. Yang, Y. Wang, S. Wang, Y. Xie, T. Wang, and G. Xiao (2020). Spatial molecular profiling: platforms, applications and analysis tools. *Briefings in Bioinformatics*.

SUPPLEMENTARY NOTES

TABLE II: List of commonly used normalization techniques for sequencing count data: ϕ is the estimated dispersion parameter for negative binomial distribution; $\sinh^{-1}(x) = \ln(x + \sqrt{1 + x^2})$ is the inverse of hyperbolic sine function.

Method	Definition
TSS	$\hat{s}_i \propto Y_i$. Each read count is divided by the total number of counts in a specific sample/location.
Q75 (Bullard et al., 2010)	$\hat{s}_i \propto q_i^{75}$. Each count is divided by the 75 th quantile of counts in a specific sample/location.
RLE (Anders and Huber, 2010)	$\hat{s}_i \propto \text{median}_j \{y_{ij} / (\prod_{k=1}^n y_{kj})^{1/n}\}$ Each read count is divided by a scale factor, measured by taking the median ratio of each sample/location to the median library.
TMM (Robinson and Oshlack, 2010)	$\hat{s}_i \propto \sum_{j=1}^p y_{ij} \exp(h_i)$ $h_i = \frac{\sum_{j \in E} w_{ij} M_{ij}}{\sum_{j \in E} w_{ij}}$ Each read count is normalized using the weighted trimmed mean of M values.
N-VST (Love et al., 2014)	Each count is transformed to stabilize variance via Naive transformation, $\tilde{y}_{ij} = \sinh^{-1}(\sqrt{\phi y_{ij}})$, followed by regressing out the log scale of total counts.
A-VST (Anscombe, 1948)	Each count is transformed to stabilize variance via Anscombe's transformation, $\tilde{y}_{ij} = \sinh^{-1}(\sqrt{\frac{y_{ij} + 3/8}{\phi - 3/4}})$, followed by regressing out the log scale of total counts.

log-VST Each count is transformed to stabilize variance via a simplified $\log(x + c)$
 (Anscombe, 1948; transformation,
 Svensson et al., $\tilde{y}_{ij} = \log(y_{ij} + (2\phi)^{-1})$,
 2018) followed by regressing out the log scale of total counts.

TABLE III: List of SV genes with spatial patterns corresponding to positive interaction parameter θ detected by BOOST-Ising: BF is the Bayes factor measuring the favor of \mathcal{M}_0 against \mathcal{M}_1 .

Gene	Bayes Factor	$2 \times \ln(\text{BF})$	Total Raw Count
Rc3h2	Inf	Inf	1174
Trib2	Inf	Inf	503
Med21	Inf	Inf	290
Nup210	Inf	Inf	163
Rsad1	Inf	Inf	94
Arap1	Inf	Inf	86
Zfp938	9999.000	18.420	190
Trim8	6665.667	17.609	809
Mrps18b	2856.143	15.914	192
Rbm15b	2499.000	15.647	151
Fam20c	2221.222	15.412	1603
Pdik1l	2221.222	15.412	143
Ccnh	951.381	13.716	1261
Erc3	951.381	13.716	239
Vapa	868.565	13.534	4017
Dgke	713.286	13.140	393
Zfp248	713.286	13.140	109

Fen1	644.161	12.936	88
Amigo2	624.000	12.872	445
Mfap3	605.061	12.811	208
Katnal1	539.541	12.581	204
Tkt	525.316	12.528	518
Plekhm3	525.316	12.528	317
Ofd1	525.316	12.528	97
Mrps24	511.821	12.476	813
Wdr3	511.821	12.476	218
Pold3	499.000	12.425	227
Rcbtb1	486.805	12.376	552
Snx21	433.783	12.145	199
Fgf14	407.163	12.018	158
Nop58	376.358	11.861	248
Zfp9	337.983	11.646	144
Bbs5	326.869	11.579	249
Eif3c	284.714	11.303	1123
Chpf2	265.667	11.164	126
Ruvbl1	262.158	11.138	470
Zfp846	262.158	11.138	103
Umps	231.558	10.890	128
"Pcnx14	226.273	10.843	286
Cstf2	214.054	10.732	780
Pias2	209.526	10.690	920
Cog4	209.526	10.690	308
Dnalc1	205.186	10.648	616
Cnih3	205.186	10.648	287

Phyhipl	203.082	10.627	1488
Hnrnpf	203.082	10.627	819
Ncoa2	195.078	10.547	953
Atg13	195.078	10.547	728
X1700025G04Rik	187.679	10.469	794
X2310003H01Rik	184.185	10.432	94
Pin1	175.991	10.341	913
Nceh1	174.439	10.323	871
Lamtor5	172.913	10.306	356
Tmem42	171.414	10.288	157
Anks3	169.940	10.271	384
Crot	167.067	10.237	481
Tbc1d23	161.602	10.170	399
Armex2	157.730	10.122	594
Nabp1	156.480	10.106	111
Rasgrp2	154.039	10.074	170

TABLE IV. Computaional time in seconds for analyzing one gene using different methods: Computation are carried out using Intel Core i5 8th Gen processors.

Methods	Computational Time
BOOST-Ising	4.53
SPARK	0.29
SpatialDE	0.067

Details of DMH algorithms

The model parameter space consists of $(\theta, \boldsymbol{\omega})$, where θ is the interaction parameter between the low and high-expressed states and $\boldsymbol{\omega} = (\omega_0, \omega_1)$ is the first-order intensity parameter. For the Ising model with external fields, the likelihood function is the conditional probability mass function $\Pr(\mathbf{p}|\theta, \boldsymbol{\omega})$, which is expressed in Equation (1).

We assigned a normal prior distribution on θ . Thus, the density function of prior distributions with a fixed hyper-parameter σ_θ^2 was

$$\pi(\theta) = \mathcal{N}(\theta; 0, \sigma_\theta^2)$$

For first-order intensity parameter $\boldsymbol{\omega} = (\omega_0, \omega_1)$, we could fix ω_1 as 1 and only estimate ω_0 , since parameters $(\theta, \omega_0, \omega_1)$ have two degrees of freedom totally. We assigned a normal prior distribution on ω_0 .

$$\pi(\omega_0) = \mathcal{N}(\omega_0; 1, \sigma_\omega^2)$$

To summarize, the full posterior can be written as

$$\pi(\theta, \omega_0|\mathbf{p}) \propto \Pr(\mathbf{p}|\theta, \boldsymbol{\omega})\pi(\theta)\pi(\omega_0)$$

Update of interaction parameter θ : To avoid calculating intractable normalizing constant, we used the DMH algorithm to update θ . Specifically, we firstly simulated a new sample θ' from $\pi(\theta)$ using the MH algorithm starting with θ . Then, we generated an auxiliary variable \mathbf{p}' through m MH updates starting with the current state \mathbf{p} and accepted

it with probability $\min(1, R_\theta)$, where,

$$R_\theta = \frac{\Pr(\mathbf{p}'|\theta, \boldsymbol{\omega})\Pr(\mathbf{p}|\theta', \boldsymbol{\omega})}{\Pr(\mathbf{p}|\theta, \boldsymbol{\omega})\Pr(\mathbf{p}'|\theta', \boldsymbol{\omega})}$$

If auxiliary variable \mathbf{p}' was accepted, update θ to θ' . Otherwise, set θ to the current value.

Update of first-order intensity parameter ω_0 : Same as updating θ , we used the DMH algorithm to update ω_0 . Specifically, we firstly simulated a new sample $\boldsymbol{\omega}' = (\omega'_0, 1)$ from $\pi(\omega_0)$ using the MH algorithm starting with ω_0 . Then, we generated an auxiliary variable \mathbf{p}' through m MH updates starting with the current state \mathbf{p} and accepted it with probability $\min(1, R_\omega)$, where,

$$R_\omega = \frac{\Pr(\mathbf{p}'|\theta, \boldsymbol{\omega})\Pr(\mathbf{p}|\theta, \boldsymbol{\omega}')}{\Pr(\mathbf{p}|\theta, \boldsymbol{\omega})\Pr(\mathbf{p}'|\theta, \boldsymbol{\omega}')}$$

If auxiliary variable \mathbf{p}' was accepted, update ω_0 to ω'_0 . Otherwise, set ω_0 to the current value.

Data generating process in simulation study

Five spatial patterns were generated as follows. Two artificial patterns are spot and linear patterns, which are shown in Figure 2(a) and (b) respectively, were on a 16×16 square lattice and had 256 spots in total. The MOB I and BC patterns, shown in Figure 2(c) and (e) respectively, were on $n = 260$ and 250 spots collected in the MOB study replicate 11 and BC study layer 2 (after filtering those spots less than 10 total counts). For MOB I and BC patterns, spots were categorized into two groups: low expression level spots (blue) and

high expression level spots (red) according to the spatial expression pattern summarized in the SPARK paper. MOB II pattern (Figure 2(d)) was also on $n = 260$ spots collected in the MOB study and the spatial distribution of spots with low expression levels and spots with high expression levels are simulated from the modified Ising model with first intensity parameters $\omega = (1, 1)$ and interaction parameter $\theta = 1$. We generated 15 SV genes and 85 non-SV genes to form a dataset under each setting. For each gene j at each location i , observed gene expression count data y_{ij} is generated from a zero-inflated negative binomial (ZINB) distribution, i.e.,

$$y_{ij} \sim \pi_i I(y_{ij} = 0) + (1 - \pi_i) \mathcal{NB}(s_i \lambda_{ij}, \phi_j)$$

where π_i are the zero-inflated rate, which means $\pi_i \times n$ spots are randomly chosen and forced as zero. $\mathcal{NB}(\mu, \phi)$ denotes the negative binomial distribution with expectation μ and dispersion $1/\phi$. In this generating process, s_i were samples from a log-normal distribution with mean 0 and standard deviation 0.2. And ϕ_j were sampled from an exponential distribution with mean 10. For the latent normalized expression level λ_{ij} , we assumed that its logarithmic scale followed normal distribution, i.e.,

$$\log(\lambda_{ij}) \sim \mathcal{N}(\beta_j + e_i, \sigma_\lambda^2)$$

Where β_j is the expression baseline of gene j and e_i is the fold-change between high expression spots and low expression spots for location i . If the gene is non-SV gene, $e_i = 0$ for all location i , which means latent normalized expression level $\log(\lambda_{ij})$ have same expectations on all spots. σ_λ is the standard deviation for random error of logarithmic scaled normalized

expression level. For SV genes with binary expressed patterns, i.e., MOB I, MOB II and BC patterns, $e_i = 0$ for low expression level spots and $e_i = \log(3)$ for high expression level spots. For SV genes with spot pattern, spots that were higher expressed than the baseline were located in the circle with the radius of 5, the value of e_i linearly decreased outward to zero from the four center points with the highest value $\log(6)$. For SV genes with linear pattern, higher expression level spots were located on the lower-right half part and the spot on bottom-right corner had the highest $e_i = \log(6)$, from where the value of e_i linearly decreased along the diagonal direction to zero.

Sensitivity analysis for data normalization methods

Table II lists seven normalization methods for sequencing data, including four methods of estimating size factor s_i , and three variance stabilizing transformation (VST) methods. We conducted a sensitivity analysis for the different normalization approaches. We simulated 10 datasets following the data generating process in the Simulation Study section. We set the zero-inflation as 30% and chose BC and MOB I patterns as expression patterns of SV genes in simulated data. We assessed the model performance with varying data normalization methods and the results were compared based on the averaged AUCs across 10 replicated datasets. Same with the simulation study, we set the criterion of SV gene identification as Bayes factor is greater than 150. The result is shown in Figure 6. BOOST-Ising is robust to the four methods - TSS, Q75, RLE and TMM. Those four methods estimate size factor s_i based on different data characteristic statistics and normalize gene expression count $\tilde{y}_{ij} = y_{ij}/s_i$. We conducted ANOVA tests on AUCs for both patterns of

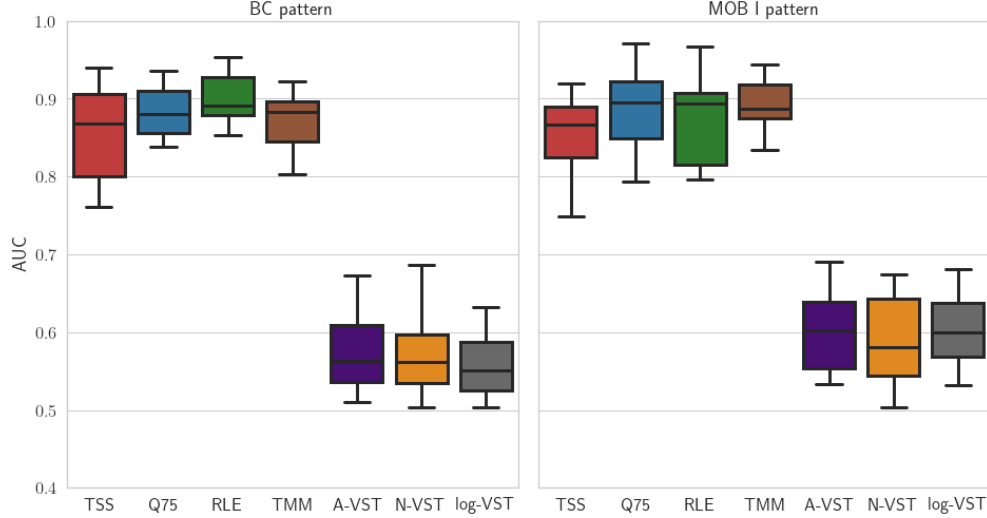


FIG. 6. Sensitivity Analysis for data normalization methods: Relationship between area under the receiver operating characteristic (ROC) curve (AUC) for identifying SV genes with the choice of different data normalization method. Each value of AUC was the averaged result of 10 simulated datasets.

these four methods and all p-values are greater than 0.05. The performance of BOOST-Ising based on three VST approaches was not satisfying. That is because VST transformed the count data to logarithmic scale, which masks the original clustered information and makes clustering methods no longer feasible. To summarize, BOOST-Ising is suitable for normalization technique $\tilde{y}_{ij} = y_{ij}/s_i$ and is not sensitive to the approaches for estimating size factor s_i .

Sensitivity analysis for clustering methods

In the Methods section, we provided two clustering approaches, K-means and Gaussian mixture clustering (GMC) for binarizing the relative expression levels. To evaluate the influence of different clustering methods, we conducted a sensitivity analysis for K-means

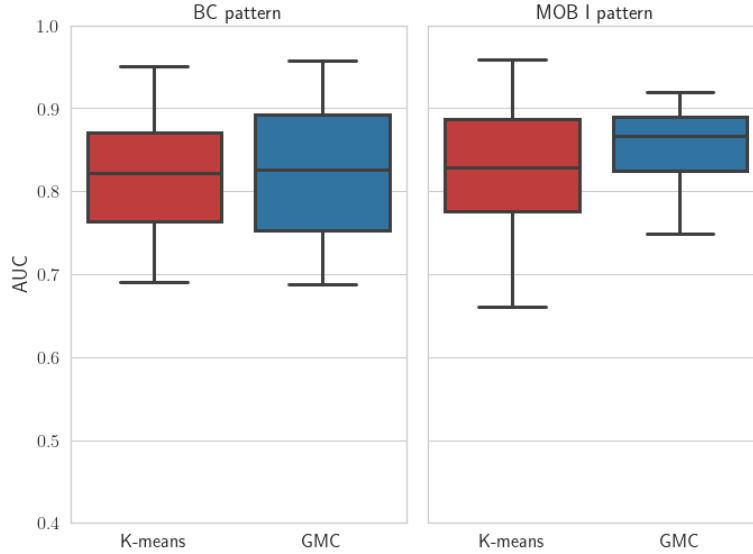


FIG. 7. Sensitivity Analysis for clustering methods: Relationship between area under the receiver operating characteristic (ROC) curve (AUC) for identifying SV genes with the choice of K-means or Gaussian mixture clustering (GMC) method when dichotomizing the relative expression levels. Each value of AUC was the averaged result of 10 simulated datasets.

and GMC. We simulated 10 datasets following the data generating process in the Simulation Study section. Same setting with the sensitivity analysis for data normalization methods, the result is shown in Figure 7. T-tests were conducted for the difference on 10 AUCs obtained from two clustering approaches under each simulation setting, and the results show that there are non-significant differences between the AUCs of these two methods (p-value=0.850 for BC pattern and 0.585 for MOB I pattern). K-means and GMC have similar performance in the BOOST-Ising for identifying SV genes, indicating that BOOST-Ising is not sensitive to the choice of clustering methods.

Sensitivity analysis for hyperparameters in the modified Ising model

We assessed the influence of setting hyperparameters in priors via sensitivity analysis. In our model, there are two hyperparameters σ_θ and σ_ω , which are the standard deviations of normal priors for interaction parameter θ and first-order intensity parameter ω_0 . To investigate model performance with respect to the choice of these hyperparameters, we simulated 10 datasets following the data generating process in Simulation Study section. We set the zero-inflation as 10% and chose MOB I pattern as the expression pattern of SV genes in simulated data. We tested the model performance with varying values of σ_θ from 1/4 to 2 and σ_ω from 1 to 100. We chose 5 values for each hyperparameter. The results given by different combinations of $(\sigma_\theta, \sigma_\omega)$ were compared based on the averaged Matthews correlation coefficient (MCC) across 10 replicated datasets. Same with simulation study, we set the criterion of SV gene identification as Bayes factor is greater than 150. The result is shown in Figure 8. Prior of ω_0 with small standard deviation σ_ω , which corresponds to informative prior, might distort the posterior inferences. Model with other settings of hyperparameters had similar performance, indicating that our model is not sensitive to the choices of hyperparameters. Based on simulation of the modified Ising model, there is a very strong spatial pattern if the absolute value of interaction parameter θ is around 1. Therefore, we choose $\sigma_\theta = 1/3$ so that around 99% percentage of values lying within the interval $(-1, 1)$ for prior of θ . In terms of the prior of ω , we choose $\sigma_\omega = 2.5$ based on the number of spots in real datasets, since this ensures a flat prior for ω .

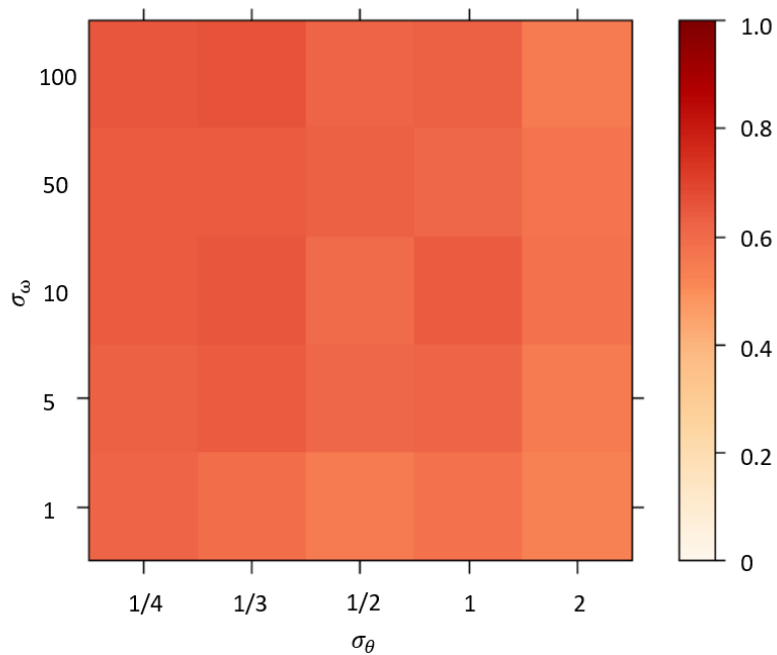


FIG. 8. Sensitivity Analysis for hyperparameters in the modified Ising model: Relationship between Matthews correlation coefficient (MCC) for identifying SV genes with the choice of $(\sigma_\theta, \sigma_\omega)$ from the normal prior on θ and ω_0 . Each value of MCC was the averaged result of 10 simulated datasets.